(3)

AFGL-TR-88-0272

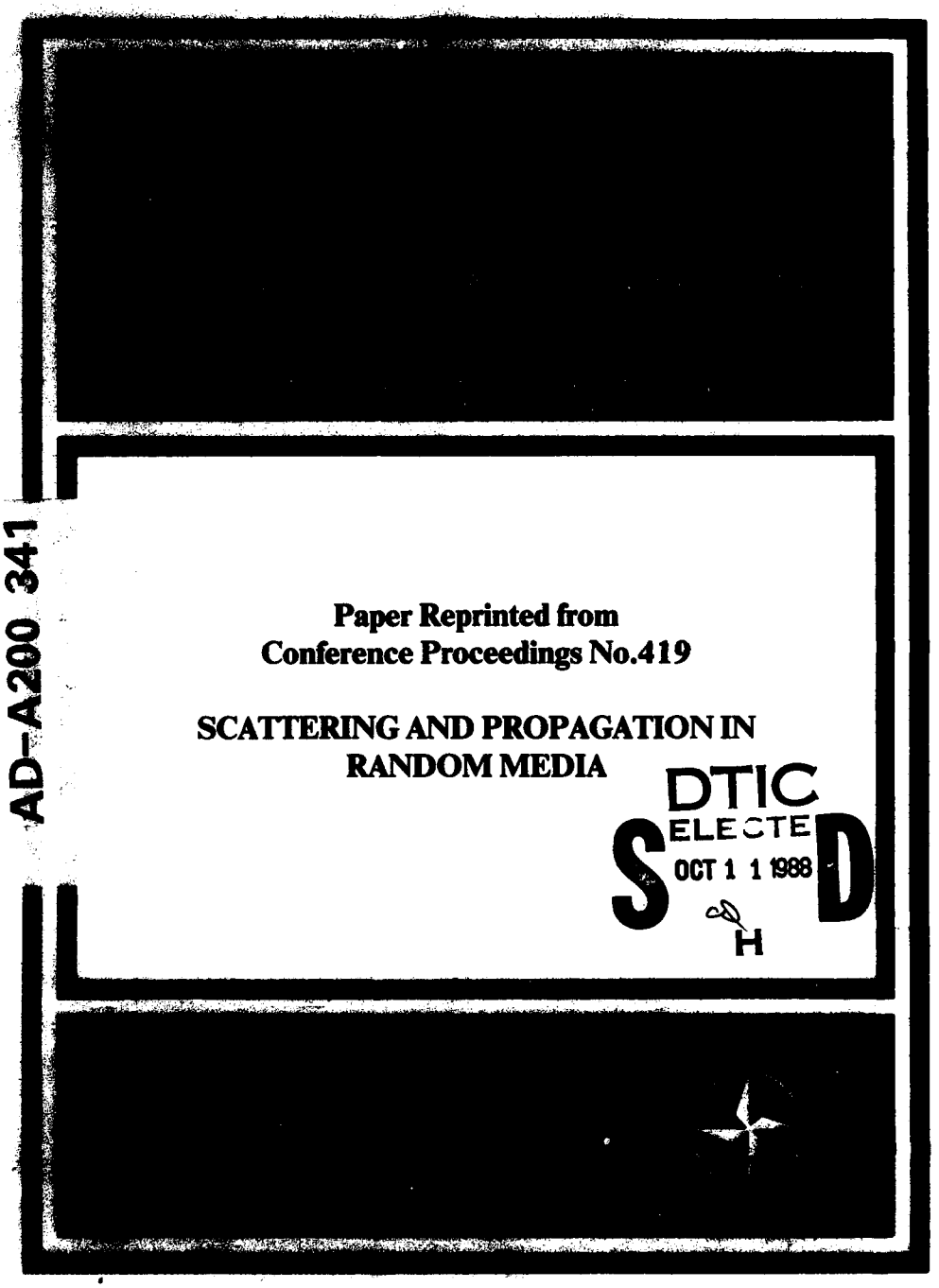

Paper Reprinted from
Conference Proceedings No.419

SCATTERING AND PROPAGATION IN RANDOM MEDIA

STRUCTURES OF DENSITY AND VELOCITY FLUCTUATIONS IN THE AURORAL OVAL AND THEIR IMPACT ON COMMUNICATION AND RADAR SYSTEMS

Sunanda Basu[1], Santimay Basu[2], W.R. Coley[3], and N.C. Maynard[2]

1 Emmanuel College, Boston MA 02115
2 Air Force Geophysics Laboratory, Hanscom AFB MA 01731
3 University of Texas at Dallas, Richardson TX 75080

SUMMARY

A new class of ionospheric irregularities in the auroral oval associated with large structured plasma flows has been recently isolated with radar and satellite in-situ measurements. These density irregularities have large power spectral densities (psd) at short scale lengths (∿ hundreds to tens of meters). The paper characterizes the density and velocity spectra in such regions and discusses their impact on scintillation observations and radar performance. The structured plasma flows may occur in association with large (∿10 μA m^{-2}) or small (∿1 μA m^{-2}) field aligned currents. The velocity spectra have fairly shallow power spectral indices (∿-1.5) in regions of large field aligned currents and are steep (∿-3) in regions of small current flows. The density spectra, on the other hand, can be described by a power law index ∿-2 in both the large and small field aligned current regions. The temporal structure of scintillations will thus be dictated not only by the scattering strength but also by the large flow velocities encountered in the auroral oval. The density structures with large psd at short scale lengths are expected to introduce considerable ionospheric clutter in HF radar systems. The effect of E-region conductivity in modifying small-scale (<1 km) F-region structure and its implication for communication and radar systems is discussed.

INTRODUCTION

In recent years a concerted effort has been made to study high latitude F-region irregularities and their relationship to bulk plasma processes. Our understanding improved significantly when it was realized that km-scale irregularity structure was associated with the steep edges of convecting large scale plasma density enhancements both in the polar cap and auroral oval (see Weber et al., 1984; 1985; Klobuchar et al., 1986 and references therein). Since the blobs are large scale features on the order of 100 km, they have long lifetimes and can be tracked by incoherent scatter radars and have been found to be convecting with the ambient plasma (Vickrey et al., 1980). The generalized ExB instability was found to be a viable mechanism for the small scale structure associated with the blobs, with magnetic field aligned currents, neutral winds, plasma drifts and the large scale blob-associated density gradients all contributing to the structure formation (see Keskinen and Ossakow, 1983 for a review of the instability processes). If radio wave propagation techniques are used as diagnostics for the blob-related irregularities, then one would see scintillation structures maximizing on the edges of total electron content (TEC) enhancements (Basu et al., 1983).

More recently, another class of F-region irregularities has been isolated which is associated with large shears in the background convective plasma flows. The unique feature of this class of irregularities is that it is not associated with organized large scale gradients of plasma density (such as to be found at the edges of blobs), but rather with velocity shears with shear gradient scale lengths of 1-10 km (Basu et al., 1987a). These irregularities are also found to have large power spectral densities (psd) at small scales (<1 km). For this reason, it is possible, for instance, to find intense scintillations without any large perturbations in TEC (Basu et al., 1986).

It is the object of this paper to present simultaneously observed density and velocity spectra obtained in the vicinity of large sheared plasma flows. Lotova (1981) has discussed the effects of velocity turbulence on the modeling of scintillations from in-situ density structure. We shall compute UHF scintillations and HF backscatter expected from such density spectral forms in the presence of considerable velocity perturbations and discuss the effect of the large convective flows on the temporal structure of scintillations observed on the ground. For comparison, we shall also compute scintillations using observed density spectra in high conductivity regions. It is found that in such regions, for example, where energetic particle precipitation is observed as in the diffuse aurora, the density spectra are fairly steep with little power at the short scales (Basu et al., 1984; 1987a). The reduced power at such scales (<100 m) is attributed to the short lifetimes of F-region irregularities in the presence of underlying E-region conductivity (Vickrey and Kelley, 1981; Heelis et al., 1985).

OBSERVED DENSITY AND VELOCITY SPECTRAL FORMS

The DE-2 satellite (Hoffman and Schmerling, 1981) is an excellent source for obtaining high resolution F-region density and velocity data at high latitudes. This data base has recently been used to make the first simultaneous measurements of density (ΔN/N) and electric field fluctuation (ΔE) spectra in the high latitude environment

(Basu et al., 1987a). It is to be noted that in low β plasma such as in the ionospheric F-region, velocity fluctuations are electrostatic and equivalent to electric field fluctuations (i.e., $\vec{v} = \vec{E} \times \vec{B}/B^2$). Thus, spectra of electric field fluctuations are to be considered equivalent to velocity fluctuation spectra.

In Figures 1(a,b) and 2(a,b) we reproduce 3 samples of 8s each density and electric field data and their respective spectra. The symbols S_H, S_G, and S_L on the data and their corresponding spectra represent samples taken from a uniformly high conductivity region (S_H), a region with sharp conductivity gradients (S_G), and a region of low conductivity (S_L). At the time the DE-2 data were taken, between 2149-2151 UT on May 26, 1982, the satellite was traversing the dawn sector of the auroral oval (0700 magnetic local time) between 70-75° invariant latitude in the southern hemisphere at an altitude of approximately 350 km. A detailed account of the particle precipitation character, small scale field aligned current intensities and ion and electron temperatures associated with these samples is given in Basu et al. (1987a).

If we confine our attention to the density and electric field data shown in Figures 1(a) and 2(a), we immediately notice the lack of high frequency structure in the high conductivity region. This is particularly noticeable in the electric field data. On the other hand, the conductivity gradient region (S_G) shows a very large amount of structure in both density and electric field, while the structure in the electric field is somewhat reduced in the low conductivity region (S_L). It is interesting to note that region S_G is associated with large field-aligned current intensities of tens of $\mu A\ m^{-2}$ in addition to the large velocity shears, whereas S_L is associated with weaker sheared flows and smaller field-aligned currents.

Before we discuss the ($\Delta N/N$) and ΔE spectra, it is important to recognize that we had to make the assumption that measurements of spatial structure in these quantities made on the satellite are Doppler shifted from zero to the frequency $f = kV_s/2\pi$, where V_s is the satellite velocity (approximately 8 km s^{-1}). In this paper whenever we refer to wavenumber k or wavelength $\lambda = 2\pi/k$, it is based upon this hypothesis. Fortunately, there is convincing evidence for this assumption of "zero-frequency turbulence" (see review by Kintner and Seyler, 1985 and references therein). Thus we feel that our assumptions concerning the spatial nature of the density and electric field variations are probably valid under most circumstances in the ULF frequency regime (Sugiura, 1984), except possibly when propagating waves such as ion cyclotron waves and Alfven waves are encountered over limited regions (Temerin, 1978; Gurnett et al., 1984).

The spectra of ($\Delta N/N$) and ΔE in the three different regimes are shown in Figures 1(b) and 2(b) respectively. Both ($\Delta N/N$) and ΔE spectra are fairly steep in the high conductivity region (S_H), while both are fairly shallow in the conductivity gradient region (S_G). Moreover, if one compares the power spectral density (psd) at 10 Hz (800 m) of the two density spectra, then one finds approximately 15 dB more power in the S_G sample than in S_H. In the ΔE spectra the separation in psd is much more dramatic with the S_G spectrum showing approximately 40 dB more power at 5 Hz (1.6 km). The density spectral forms and psd in the S_L and S_G regimes are almost identical with power law slopes of ~-2. However, the slopes of the ΔE spectra in the S_L and S_G regimes are quite different with the S_L spectral slope being -3 compared to the S_G slope of shallower than -2. In all 3 situations, the important point to note is that the electric field (i.e., velocity) spectra are either equal in slope or steeper than the corresponding density spectra. Thus following the arguments of Lotova (1981), it is expected that we should be able to model scintillations from in situ density measurements. However, the large background velocities (100 mV m^{-1} is equivalent to 2 km s^{-1} convection velocities) would significantly alter the temporal structure of scintillations.

SCINTILLATION ESTIMATES

It is possible to estimate scintillations in the weak scatter formulation (Rino, 1979) if the irregularity amplitude, density spectral forms, background densities and irregularity layer thickness are known. It is the object of this paper to present several estimates of scintillations that may be observed under solar maximum or minimum conditions.

We use the density spectra observed in the velocity shear regions to estimate the scintillations to be expected with different levels of background ionization. We note from the top two panels of Figure 1b that the psd is -18 dB at a frequency of 1 Hz. Using the satellite velocity of 8 km s^{-1}, this frequency is equivalent to a scale length of 8 km. We use the measured psd and the observed one-dimensional density spectral slope of -2 to compute intensity scintillations at 413 MHz which is the UHF frequency transmitted by the orbiting HiLat satellite. We utilized the observed irregularity amplitude of approximately 20 percent and a thickness of 100 km for the irregularity layer. The latter seems to be a good estimate if contours of maximum density in the F-region are studied using latitude/altitude scans made by incoherent scatter radars at auroral latitudes (Basu et al., 1986). The weak-scatter formulation of Rino (1979) was used for the purpose. The equation for the S_4 index (Briggs and Parkin, 1963) is given by:

$$S_4^2 = (r_e\lambda)^2\ (L \sec\theta)\ C_S\ Z^{\nu-\frac{1}{2}}\ f(\nu)\ J$$

where r_e - classical radius of the electron
λ - the radio wavelength
L - the thickness of the irregularity layer

θ - the ionospheric zenith angle
C_S - strength of turbulence
Z - $\lambda z_R \sec\theta/4\pi$, z_R is the range
ν - related to 1-D spectral index given by $2\nu-1$
J - geometrical parameter related to irregularity anisotropy
$f(\nu)$ - a function of the irregularity spectral index involving Γ-functions.

In this paper, we shall confine our computations to the S_4 index only as it is uniquely defined by the measurement of C_S and ν, the only major assumption being in regard to the irregularity anisotropy. The phase scintillation index, on the other hand, depends on the detrend filter characteristics and the effective velocity of the ray path. Since we will be primarily considering auroral observations, we will assume sheet-like irregularities aligned with the local L-shell (Rino et al., 1978). The best estimates of the shape is given by 8:4:1, with the largest anisotropy being along the magnetic field (Fremouw and Secan, 1984). The effect of the irregularity anisotropy on the S_4 index, in particular, is minimal except for regions of exact alignment.

In general, the greatest degree of variability is observed in C_S which is the strength of turbulence (Fremouw and Secan, 1984). The in-situ DE-2 data thus gives us an estimate of this important parameter for scintillation computations. As noted earlier the measured psd of -18 dB, the spectral index of -2 and irregularity amplitude of 20 percent translates to a value of $C_S = 4 \times 10^{-19}$ mks units using equations given by Rino (1979). This value of C_S translates to $S_4 = 0.25$ at 413 MHz for near overhead locations at an auroral station such as Tromso, Norway (magnetic dip = 78°). If field alignment is considered, then the S_4 index ≈ 0.5. Needless to say, at such times the S_4 index at 137 MHz will be saturated and cannot be estimated using this weak-scatter formulation.

It is gratifying to note, that these computations agree well with the HiLat observations at 413 MHz made at Tromso shown in Figure 3. The irregularities during this event were associated with velocity shears (Basu et al., 1986). Two significant structures were observed both giving rise to saturated VHF scintillations. However, the UHF S_4 index is slightly less than 0.3 for one and 0.4 for the other which is in the geometrical enhancement region. It is interesting to note that the background density at this time was 3×10^{11} m^{-3} as compared to 2×10^{11} m^{-3} used in the computations based on DE-2 data. This indicates that large irregularity amplitudes coupled with relatively shallow slopes can cause significant UHF scintillations in the auroral oval. Further, when the background density is larger by a factor of 3 or 4 during high sunspot conditions, if the same irregularity amplitude is preserved, it is possible to have a three to four-fold increase in the scintillation level. Thus saturated 413 MHz and even significant 1 GHz scintillation may be expected in the auroral oval in conjunction with velocity shears with particularly intense events being observed in the geometrical enhancement region.

EFFECT OF UNDERLYING E-REGION CONDUCTIVITY ON SCINTILLATIONS

The bottom panel of Figure 1a shows density data (S_H) obtained by DE-2 in the presence of diffuse auroral precipitation which creates high conductivity in the E-region. The field-line integrated Pedersen conductivity is 10 mhos and the Hall conductivity is 40 mhos (Basu et al., 1987a). The corresponding spectrum in Figure 1b shows the spectral slope to be -2.5. The electric field spectrum shown in Figure 2b is even steeper. Figure 4 shows spectral data in the auroral oval obtained from AE-D which exhibits a one-dimensional spectral slope of -3 in the scalelength range smaller than 1 km which is the region of interest for UHF scintillations (Basu et al., 1984). In order to emphasize the effect of a conducting E-region, we choose this experimentally observed slope of -3 in association with the large irregularity amplitude of 20 percent which was observed in conjunction with the velocity shears discussed earlier. Using exactly the same background density and anisotropy parameters, we obtain $C_S = 8 \times 10^{-15}$ mks units and $S_4 = .05$ in the high conductivity region using a spectral index of -3. This is a fairly startling result which shows that scintillation is reduced by a factor of 5 for the same irregularity amplitude and F-region density merely by going into a region whose magnetic field lines terminate in a conducting E-region. Vickrey and Kelley (1982) and Heelis et al. (1985) have studied the effect of E-region conductivity on lifetimes of irregularities and we point out here how such factors can have a large impact on communication systems. The upshot is that it is difficult to observe significant UHF scintillations in regions of high E-region conductivity. This is an important factor to contend with in the auroral oval and polar cap, the former being the seat of the energetic auroral precipitation and the latter being illuminated by solar radiation continuously in the summer months. Indeed intensity scintillation measurements at Thule, Greenland in the polar cap conducted over half a solar cycle (1979 - 1984) have shown the enormous decrease of scintillation occurrence and magnitude during the local summer (Basu et al., 1987b).

EFFECT OF LARGE VELOCITIES ON SCINTILLATION STRUCTURE

Figure 2 gives examples of intense small scale velocity structure with 100 mV m^{-1} electric field giving rise to a velocity of 2 km s^{-1} in the high latitude environment. However, at other times fairly steady velocities on the order of 1 km s^{-1} may be observed in the anti-sunward direction in the polar cap and in the E-W direction in auroral latitudes (Weber et al., 1984; Basu et al., 1983). Such enhanced convection velocities have a noticeable effect on the temporal structure of scintillations as

manifested by measured decorrelation times, intensity spectral shapes and the intensity rate of scintillations. We present intensity scintillation data at 250 MHz in Figure 5 from two consecutive days as observed at Goose Bay within the auroral oval (Basu et al., 1985). Significant scintillations of the same level were observed on both days, but on March 7 the decorrelation time shown in dotted lines was found to be 2 s while that on March 8 was 0.4 s. Estimates of the velocity could be obtained from the intensity scintillation spectra at the 2 times denoted by arrows on Figure 5. These two spectra are shown in Figure 6. The spectrum on March 7 shows a Fresnel frequency (f_F) of 0.05 Hz while it is 0.3 Hz on March 8. Using the relationship $f_F = u/(2\lambda z)^{\frac{1}{2}}$ where u is the drift velocity perpendicular to the ray path (mostly E-W for this geometry), we determine this drift to be 65 m s^{-1} on March 7 and 390 m s^{-1} on March 8. Furthermore, we note that this velocity variation gives rise to widely different intensity rates. For the data sets shown in Figure 5 the intensity rate of 3 dB s^{-1} occurs in 0.1 percent of the total population on March 7; while the rate becomes 7 dB s^{-1} on March 8 for the same 0.1 percent level as shown in Figure 7 (Basu et al., 1987b). Again we find the variation of a magnetospheric parameter, namely its convection velocity, having a significant impact on propagation systems operating at high latitudes. Phase scintillations were not discussed in this paper, but it was shown by Basu et al. (1985) that enhanced convection yields large values of phase scintillation when the source is a geostationary satellite. Thus convection not only affects second order quantities, such as decorrelation time, but even affects first order quantities, such as phase scintillation magnitude.

EFFECT OF UNDERLYING E-REGION CONDUCTIVITY ON F-REGION RADAR SYSTEM OPERATING AT HF

It was mentioned by Basu et al. (1987a) that one of the unique characteristics of velocity-shear-associated irregularities was the existence of high psd of $(\Delta N/N)$ all the way up to approximately 10 m scalelength. In Figure 8 we show the psd at 125 m and 46.5 m observed in conjunction with the three categories of spectra displayed in Figures 1 and 2. We note from Figure 8 that the psd associated with S_H is almost three orders of magnitude less than that observed in the velocity shear region indicated by S_G and S_L. The filter output at 17 m, while not shown, indicates a similar variation of psd between the two categories, that in the high conductivity region being 10^{-11} Hz^{-1} whereas it is 10^{-8} Hz^{-1} in shear regions. Now, an HF radar operating at 10 MHz will be sensitive to a scalelength of 15 m. Since the background density variation through the region encompassing S_H, S_G and S_L in Figure 8 is insignificant, and since coherent radar backscatter is proportional to $(\Delta N)^2$ (Woodman and Basu, 1978), we can expect a 30 dB decrease in radar returns from the F-region at 10 MHz when the radar beam sweeps into the high conductivity region from the velocity shear region. Indeed Baker et al. (1986) have shown that HF radar backscatter has been significant from the cusp region which is a seat of large velocity shears and where E-region conductivity is low because of the soft particle precipitation. Thus, we find that underlying E-region conductivity controls, to a great extent, the evolution of F-region structure, and this in turn has significant impact on radar and communication systems operating in the high latitude environment.

REFERENCES

Baker, K.B., R.A. Greenwald, A.D.M. Walker, P.F. Bythrow, L.J. Zanetti, T.A. Potemra, D.A. Hardy, F.J. Rich, and C.L. Rino, A case study of plasma processes in the dayside cleft, J. Geophys. Res., 91, 3130, 1986.

Basu, Su., E. MacKenzie, S. Basu, H.C. Carlson, D.A. Hardy, F.J. Rich, and R.C. Livingston, Coordinated measurements of low-energy precipitation and scintillation/TEC in the auroral oval, Radio Sci., 18, 1151, 1983.

Basu, Su., S. Basu, E. MacKenzie, W.R. Coley, W.B. Hanson, and C.S. Lin, F-region electron density irregularity spectra near auroral acceleration and shear regions, J. Geophys. Res., 89, 5554, 1984.

Basu, Su., S. Basu, E. MacKenzie, and H.E. Whitney, Morphology of phase and intensity scintillations in the auroral oval and polar cap, Radio Sci., 20, 347, 1985.

Basu, Su., S. Basu, C. Senior, D. Weimer, E. Nielsen, and P.F. Fougere, Velocity shears and sub-km scale irregularities in the nighttime auroral F-region, Geophys. Res. Lett., 13, 101, 1986.

Basu, Su., S. Basu, E. MacKenzie, P.F. Fougere, W.R. Coley, N.C. Maynard, J.D. Winningham, M. Sugiura, W.B. Hanson, and W.R. Hoegy, Simultaneous density and electric field fluctuation spectra associated with velocity shears in the auroral oval, Submitted to J. Geophys. Res., 1987a.

Basu, S., E. MacKenzie, Su. Basu, E. Costa, P.F. Fougere, H.C. Carlson, and H.E. Whitney, 250 MHz/GHz scintillation parameters in the equatorial, polar and auroral environments, IEEE Journal on Selected Areas in Communications, SAC-5, 102, 1987b.

Briggs, B.H. and I.A. Parkins, On the variation of radio star and satellite scintillation with zenith angle, J. Atmos. Terr. Phys., 25, 339, 1963.

Fremouw, E.J. and J.A. Secan, Modeling and scientific application of scintillation results, Radio Sci., 19, 687, 1984.

Gurnett, D.A., R.L. Huff, J.D. Menietti, J. L. Burch, J.D. Winningham, and S.D. Shawhan, Correlated low-frequency electric and magnetic noise along the auroral field lines, J. Geophys. Res., 89, 8971, 1984.

Heelis, R.A., J.F. Vickrey, and N.B. Walker, Electrical coupling effects on the temporal evaluation of F-layer plasma structure, J. Geophys. Res., 90, 437, 1985.

Hoffman, R.A. and E.R. Schmerling, Dynamics Explorer program: an overview, Space Sci. Instr., 5, 345, 1981.

Keskinen, M.J. and S.L. Ossakow, Theories of high-latitude ionospheric irregularities: a review, Radio Sci., 18, 1077, 1983.

Kintner, P.M. and C.E. Seyler, The status of observations and theory of high latitude ionospheric and magnetospheric plasma turbulence, Space Sci. Rev., 41, 91, 1985.

Klobuchar, J.A., G.J. Bishop, and P.H. Doherty, Total electron content and L-band amplitude and phase scintillation measurements in the polar cap ionosphere, AGARD Conference Proceeding No. 382, Propagation Effects on Military Systems in the High Latitude Region, June 1985.

Lotova, N.A., Temporal scintillation spectra with allowance for the solar wind velocity distribution. Theory, Geomagnetism and Aeronomy, 21, 447, 1981.

Rino, C.L., A power-law phase screen model for ionospheric scintillation. (1) Weak scatter, Radio Sci., 14, 1135, 1979.

Rino, C.L., R.C. Livingston, and S.J. Matthews, Evidence for sheet-like auroral ionospheric irregularities, Geophys. Res. Lett., 5, 1039, 1978.

Sugiura, M., A fundamental magnetosphere-ionosphere coupling mode involving field-aligned currents as deduced from DE-2 observation, Geophys. Res. Lett., 11, 877, 1984.

Temerin, M., The polarization, frequency, and wavelengths of high-altitude turbulence, J. Geophys Res., 83, 2609, 1978.

Vickrey, J.F. and M.C. Kelley, The effects of a conducting E-layer on classical F-region cross-field plasma diffusion, J. Geophys. Res., 87, 4461, 1982.

Vickrey, J.F., C.L. Rino, and T.A. Potemra, Chatanika/TRIAD observations of unstable ionization enhancements in the auroral F-region, Geophys. Res. Lett., 7, 789, 1980.

Weber, E.J., J. Buchau, J.G. Moore, J.R. Sharber, R.C. Livingston, J.D. Winningham, and B.W. Reinisch, F-layer ionization patches in the polar cap, J. Geophys. Res., 89, 1683, 1984.

Weber, E.J., R.T. Tsunoda, J. Buchau, R.E. Sheehan, D.J. Strickland, W. Whiting, and J.G. Moore, Coordinated measurements of auroral zone plasma enhancements, J. Geophys. Res., 90, 6497, 1985.

Woodman, R.F. and Su. Basu, Comparison between in-situ spectral measurements of equatorial F-region irregularities and backscatter observations at 3m wavelength, Geophys. Res. Lett., 5, 869, 1978.

ACKNOWLEDGMENT

The work at Emmanuel College was supported by AFGL Contract F19628-86-K-0038.

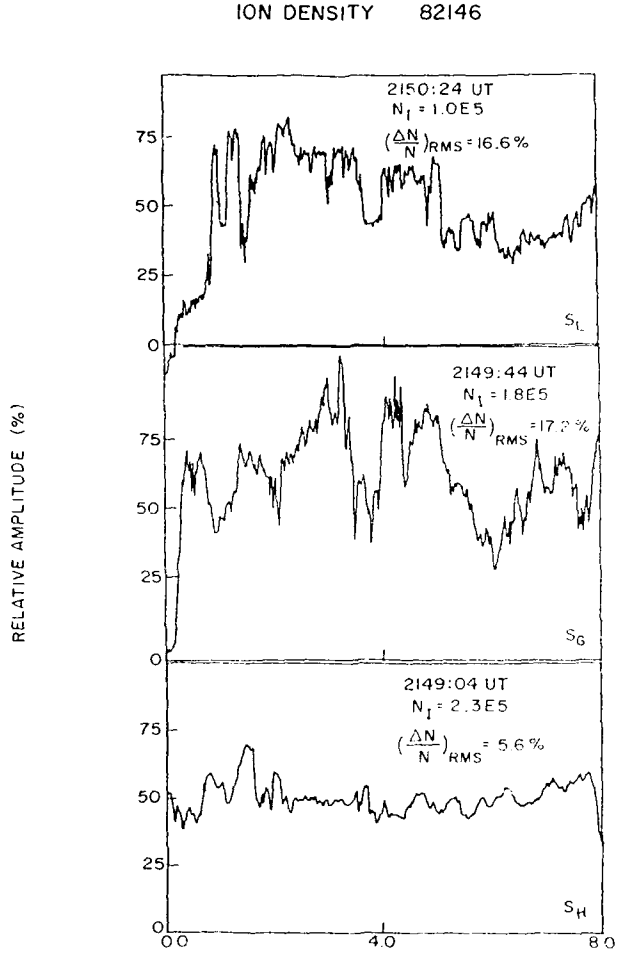

Figure 1a. Three 8-s samples of high resolution (64 Hz) density data from DE-[illegible] in high conductivity region (S_H), high gradient in the conductivity [illegible] (S_G) and low conductivity region (S_L). The irregularity amplitudes are indicated on the respective diagrams.

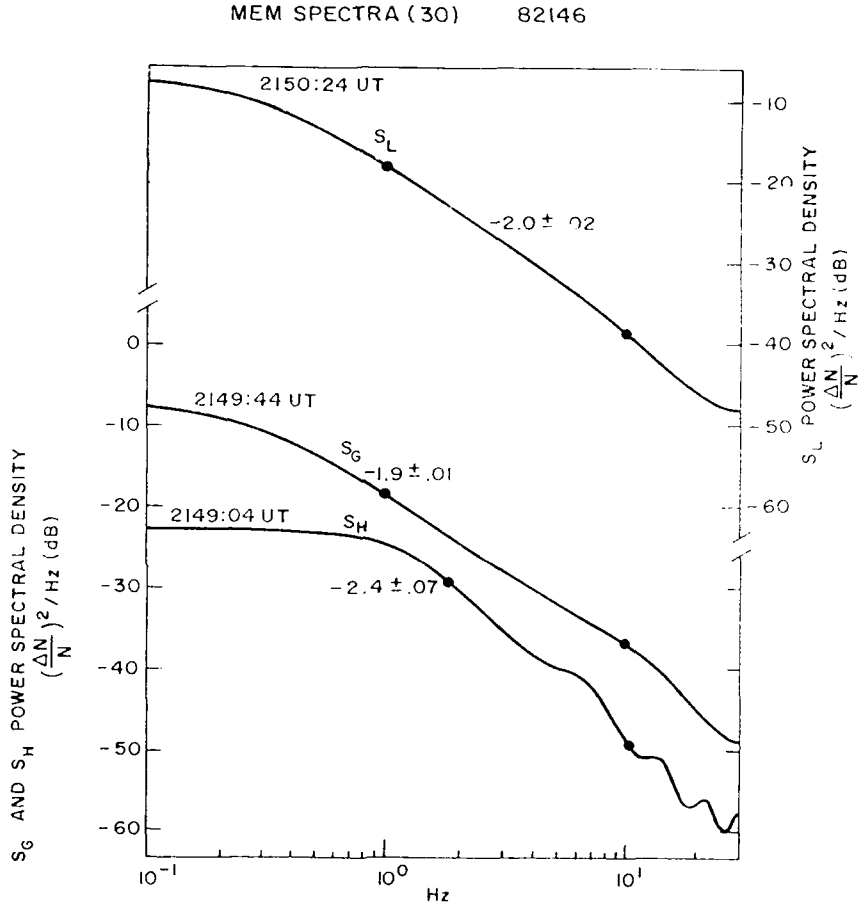

Figure 1b. Maximum entropy spectra corresponding to the three 8-s samples of Jensen's data shown in Figure 1a. The spectral indices are indicated on the respective diagrams.

DC ELECTRIC FIELD 82146

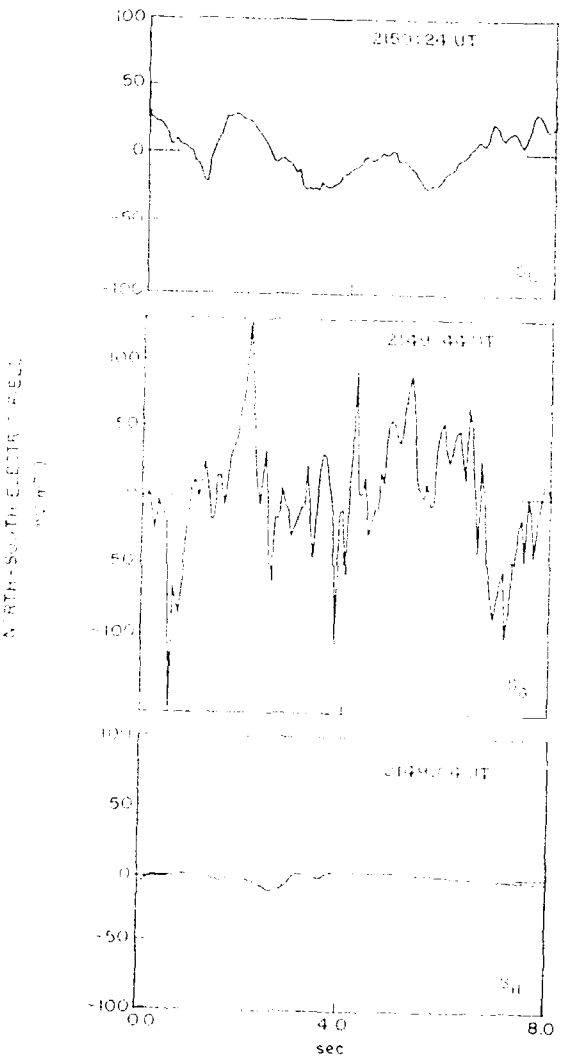

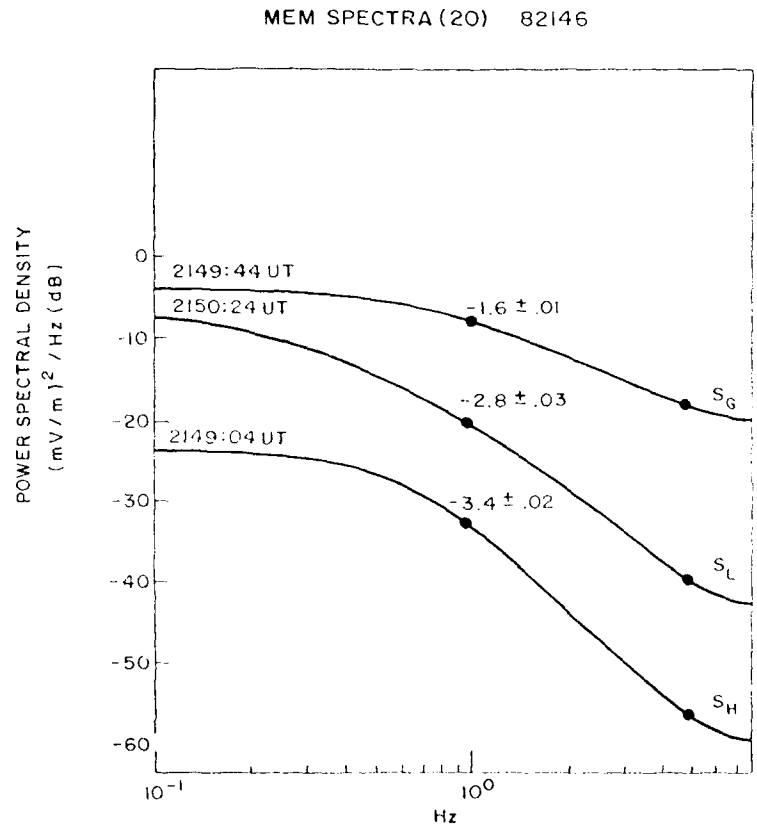

Figure 2b. Maximum entropy spectra corresponding to the three 8-s samples of electric field data shown in Figure 2a. The times are the same as those for Figures 1(a & b). Note that the spectrum for 2150:24 UT is shown in the middle panel.

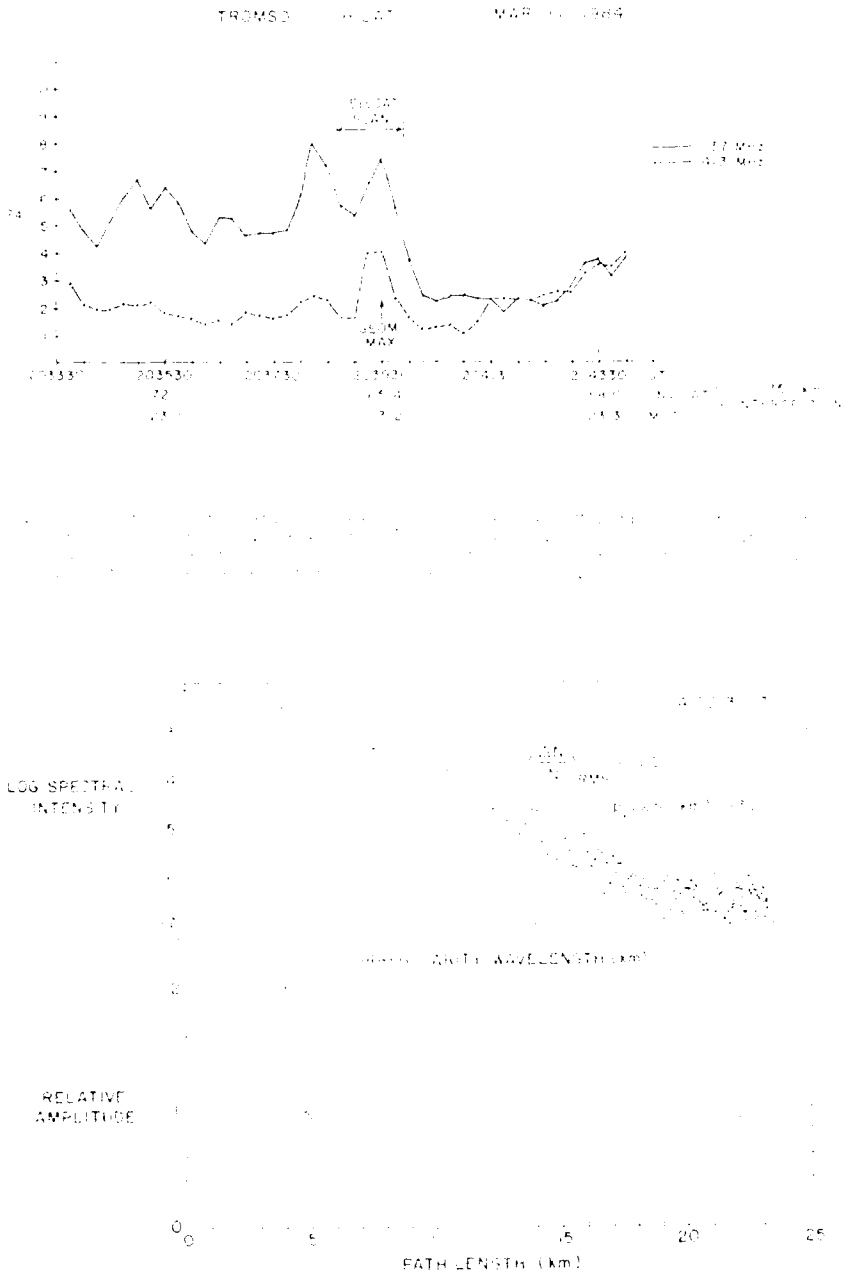
LOG SPECTRAL INTENSITY
RELATIVE AMPLITUDE
PATH LENGTH (km)

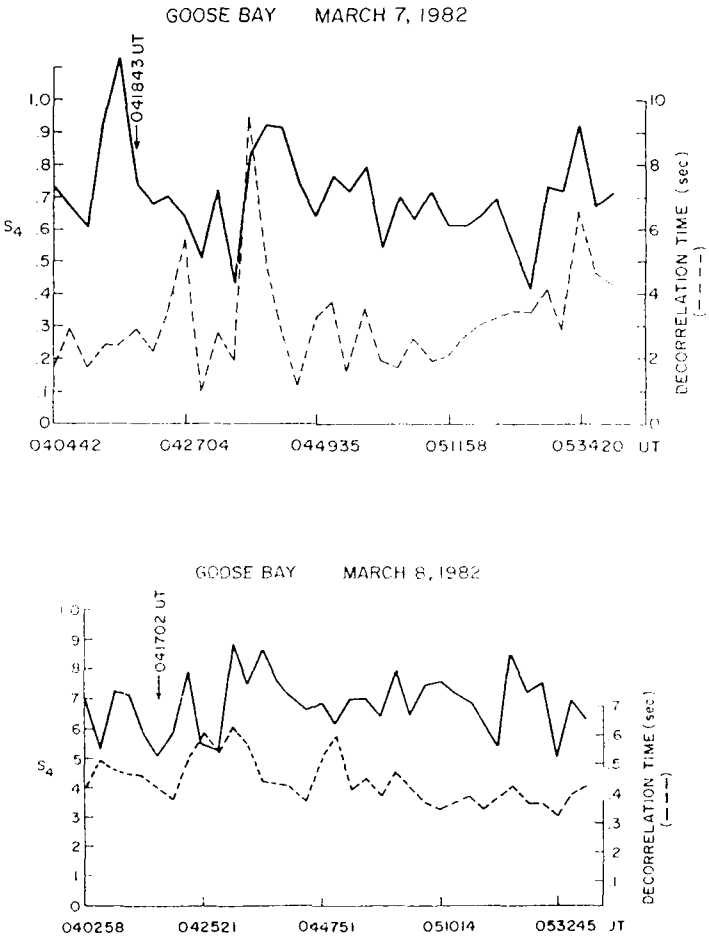

Figure 5. Intensity scintillation index S_4 at 250 MHz observed at Goose Bay on March 7 and March 8, 1982. Decorrelation times are also shown. Note the great variation in decorrelation time from one day to the next even though S_4 level is similar.

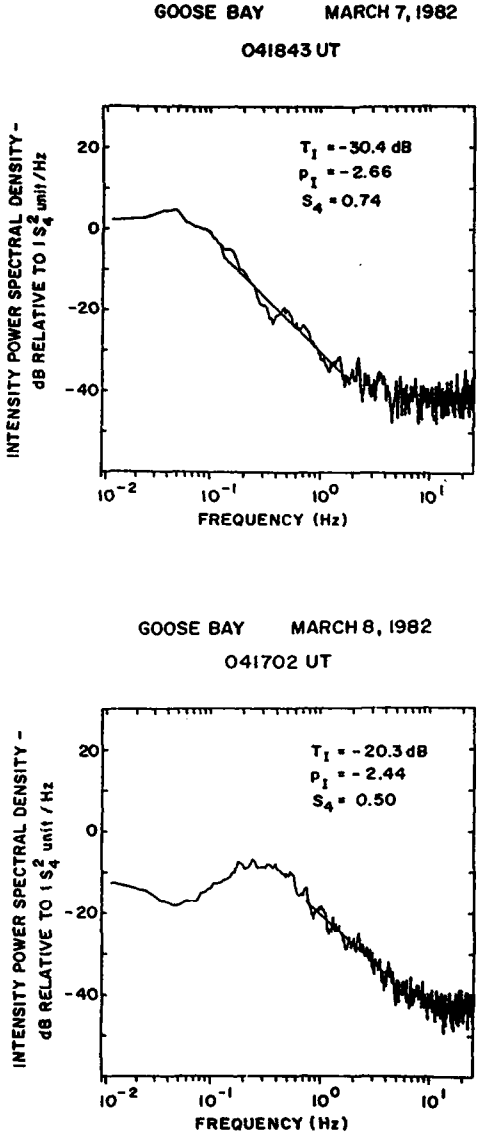

Figure 6. Intensity scintillation spectra observed on March 7 and March 8 at times denoted by arrows on Figure 5. Note the great variation in Fresnel frequency of these two spectra.

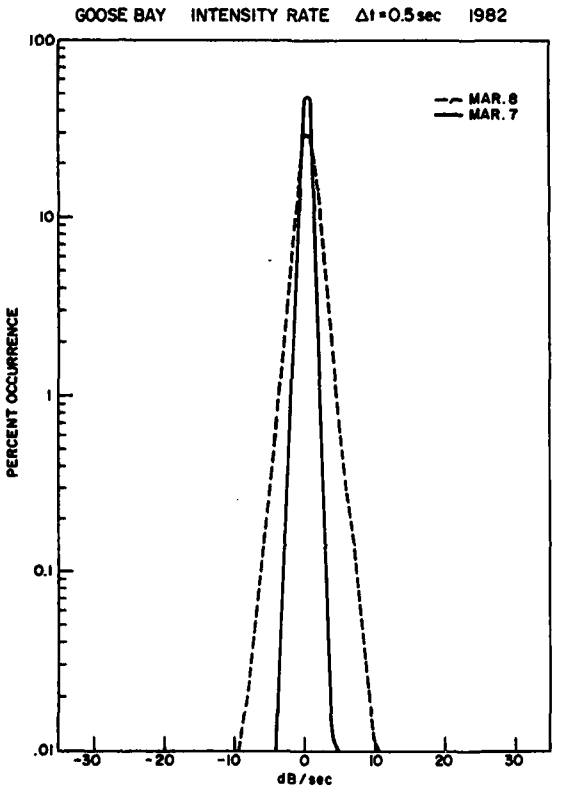

Figure 7. The distribution of intensity rate of scintillations for the data shown in Figure 5. The drift was six times larger on March 8 as compared to March 7.

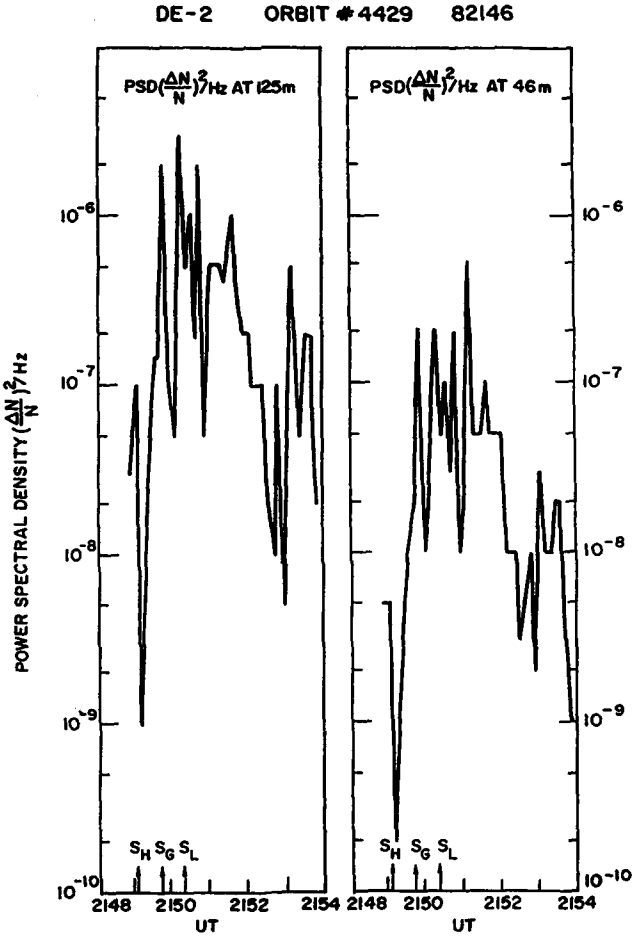

Figure 8. The power spectral density at 125 m and 46.5 m from DE-2 data. S_H, S_G and S_L have the same meaning as in Figures 1 and 2.

Unclassified
SECURITY CLASSIFICATION OF THIS PAGE

AD-A190 841

REPORT DOCUMENTATION PAGE

1a. REPORT SECURITY CLASSIFICATION: Unclassified	1b. RESTRICTIVE MARKINGS: None
2a. SECURITY CLASSIFICATION AUTHORITY	3. DISTRIBUTION/AVAILABILITY OF REPORT: Approved for public release; distribution unlimited.
2b. DECLASSIFICATION/DOWNGRADING SCHEDULE	
4. PERFORMING ORGANIZATION REPORT NUMBER(S)	5. MONITORING ORGANIZATION REPORT NUMBER(S): AFGL-TR-88-0272
6a. NAME OF PERFORMING ORGANIZATION: Emmanuel College; 6b. OFFICE SYMBOL (If applicable)	7a. NAME OF MONITORING ORGANIZATION: Air Force Geophysics Laboratory
6c. ADDRESS (City, State and ZIP Code): 400 The Fenway, Boston MA 02115	7b. ADDRESS (City, State and ZIP Code): Hanscom AFB, Massachusetts 01731
8a. NAME OF FUNDING/SPONSORING ORGANIZATION; 8b. OFFICE SYMBOL (If applicable)	9. PROCUREMENT INSTRUMENT IDENTIFICATION NUMBER: F19628-86-K-0038
8c. ADDRESS (City, State and ZIP Code)	10. SOURCE OF FUNDING NOS.

PROGRAM ELEMENT NO.	PROJECT NO.	TASK NO.	WORK UNIT NO.
62101F	4643	09	AH

11. TITLE (Include Security Classification): Structures of Density ... (see reverse)

12. PERSONAL AUTHOR(S): Sunanda Basu, Santimay Basu*, W.R. Coley**, and N.C. Maynard*

13a. TYPE OF REPORT	13b. TIME COVERED	14. DATE OF REPORT (Yr., Mo., Day)	15. PAGE COUNT
Scientific Report #1	FROM 10/2/86 TO 4/30/87	1987 July	14

16. SUPPLEMENTARY NOTATION
*AFGL, Hanscom AFB, MA 01731; **UTD, Richardson, TX 75080.
Paper reprinted from AGARD Conference Proceedings No. 419, May, 1987.

17. COSATI CODES		
FIELD	GROUP	SUB. GR.

18. SUBJECT TERMS (Continue on reverse if necessary and identify by block number)
Density spectra; velocity spectra; auroral scintillations; radar backscatter; E-region conductivity

19. ABSTRACT (Continue on reverse if necessary and identify by block number)

A new class of ionospheric irregularities in the auroral oval associated with large structured plasma flows has been recently isolated with radar and satellite in-situ measurements. These density irregularities have large power spectral densities (psd) at short scale lengths (~ hundreds to tens of meters). The paper characterizes the density and velocity spectra in such regions and discusses their impact on scintillation observations and radar performance. The structured plasma flows may occur in association with large (~10 $\mu A\ m^{-2}$) or small (~1 $\mu A\ m^{-2}$) field aligned currents. The velocity spectra have fairly shallow power spectral indices (~-1.5) in regions of large field aligned currents and are steep (~-3) in regions of small current flows. The density spectra, on the other hand, can be described by a power law index ~-2 in both the large and small field aligned current regions. The temporal structure of scintillations will thus be dictated not only by the scattering strength but also by the large flow velocities
(continued on reverse)

20. DISTRIBUTION/AVAILABILITY OF ABSTRACT	21. ABSTRACT SECURITY CLASSIFICATION
UNCLASSIFIED/UNLIMITED ☒ SAME AS RPT. ☐ DTIC USERS ☐	Unclassified

22a. NAME OF RESPONSIBLE INDIVIDUAL	22b. TELEPHONE NUMBER (Include Area Code)	22c. OFFICE SYMBOL
William K. Vickery	(617) 377-3220	AFGL/LIS

DD FORM 1473, 83 APR — EDITION OF 1 JAN 73 IS OBSOLETE.

Unclassified
SECURITY CLASSIFICATION OF THIS PAGE